CloudSat measurements of landfalling hurricanes Gustav and Ike (2008)

Sergey Y. Matrosov[1]

Received 17 May 2010; revised 17 August 2010; accepted 24 August 2010; published 8 January 2011.

[1] The spaceborne 94 GHz radar onboard the CloudSat polar orbiting satellite offers new opportunities in estimating parameters of precipitating cloud systems including hurricanes. CloudSat measurements can resolve the vertical extent of storms and hurricanes, thus providing a view of their complex structure. These measurements can be used to retrieve with high spatial resolution rainfall and ice content parameters in an atmospheric vertical column as the satellite moves over the precipitating systems. Two major Atlantic hurricanes of the 2008 season, Gustav and Ike, were observed by CloudSat near their landfalls on the coast of the Gulf of Mexico. CloudSat measurements indicated cloud top heights at around 14–16 km above the ground and extended areas of startiform-like precipitation with estimated rain rates in a range of about 3–12 mm h^{-1}. The radar bright band features observed just below the freezing level were identifiable for most measured reflectivity profiles. Maximum retrieved ice water path values reached about 20,000 g m^{-2}. CloudSat rain rate retrievals over land and water agreed reasonably well with approximately coincident estimates from surface precipitation radars in the areas where measurements from these radars were available and were not contaminated by melting layer returns. Hurricane Gustav remnants observed by CloudSat several days after the landfall were characterized by smaller values of rain rate and ice water path (~2–3 mm h^{-1} and 1000–10,000 g m^{-2}, correspondingly). The hurricane parameters retrieved from CloudSat measurements may complement data from other satellite sources, which are traditionally used for hurricane observations.

Citation: Matrosov, S. Y. (2011), CloudSat measurements of landfalling hurricanes Gustav and Ike (2008), *J. Geophys. Res.*, *116*, D01203, doi:10.1029/2010JD014506.

1. Introduction

[2] While different visible, infrared and microwave satellite remote sensors have been successfully used for observations of hurricanes for several decades, the first spaceborne W band (94 GHz) cloud profiling radar (CPR) [*Tanelli et al.*, 2008] onboard the CloudSat satellite, which was launched in 2006, provides some new possibilities for retrievals of hurricane properties. The first several years of CloudSat operations yielded valuable information about global cloud properties [e.g., *Stephens et al.*, 2008]. Although providing quantitative information about nonprecipitating clouds is the main objective of the CloudSat project, CPR measurements can also be used for retrieving parameters of precipitating systems [e.g., *Matrosov*, 2007; *Mitrescu et al.*, 2010]. The CPR is often able to "see" through precipitating cloud systems and detect the attenuated ground return. In such cases, the path-integrated attenuation (PIA) approach was devised to estimate mean layer rain rate [*Haynes et al.*, 2009]. This approach usually works better for lighter rainfall which is observed over water surfaces.

[3] Another approach for stratiform rain retrievals is based on relating the height derivatives of observed CPR reflectivities to rain rate [*Matrosov*, 2008, 2010a]. This approach does not require the surface returns and can be used for more intense rainfall over both land and water surfaces. Because of the high sensitivity (~−28 dBZ) and low attenuation in the ice cloud phase, the CPR is able to observe the vertical extent of thick precipitating cloud systems including hurricanes, although backscatter from rainfall regions is much attenuated and ground returns sometimes are not detected. The echoes from the rain layer, however, are still present, although they are influenced by multiple scattering. Attenuation effects are the main source of information for rainfall retrievals based on the height derivatives of CPR reflectivities.

[4] The ability of the CPR to provide information about hurricanes has been realized in the community [e.g., *Mitrescu et al.*, 2008; *Durden et al.*, 2009]. In one earlier study showing the utility of CloudSat to hurricane studies, *Luo et al.* [2008] showed that the cloud top heights from CPR estimates

[1]Cooperative Institute for Research in Environmental Sciences, University of Colorado and NOAA/Earth System Research Laboratory, Boulder, Colorado, USA.

0148-0227/11/2010JD014506

combined with brightness temperatures from other A-train satellite constellation sensors could be used for estimating hurricane intensity. The CloudSat tropical cyclone overpass archive is maintained by the Colorado State University (http://reef.atmos.colostate.edu/~natalie/tc/).

[5] The purpose of this study is to outline the possibilities of CloudSat measurements to provide quantitative information on the rainfall and ice cloud components in hurricanes. Two major hurricanes (i.e., Gustav and Ike) of the 2008 season which reached the continental United States were chosen for illustrations. The choice of landfalling hurricanes in this study was dictated, in part, due to the availability of independent rainfall observations from the surface precipitation radars, which are the important source of information about hurricanes over the land areas [e.g., *Skwira et al.*, 2005]. Another reason for this choice is that landfalling hurricanes have a high societal impact and their properties are subject of many model studies [e.g., *Tuleya et al.*, 1984; *Chen and Yau*, 2003; *Kimball*, 2008]. The CloudSat-based retrievals of hurricane characteristics may in future provide useful validation information for such studies.

[6] Current quantitative satellite techniques often use passive multichannel microwave measurements and/or the Tropical Rainfall Measuring Mission (TRMM) K_u band (13.8 GHz) scanning precipitation radar (PR) for estimating rainfall [e.g., *Lonfat et al.*, 2004; *Yokoyama and Takayabu*, 2008]. These techniques work better for observations over water surfaces. While CloudSat approaches obviously cannot substitute for the existing satellite techniques, the CloudSat-based estimates can be a useful additional source of information about hurricane properties. Some advantages of CloudSat approaches include the availability of high spatial resolution coupled rainfall and ice cloud information and the possibility of retrievals over both land and water surfaces with similar accuracies, thus allowing one to track possible hurricane property changes during landfall. One significant limitation of CloudSat observations is, however, a lack of significant spatial coverage available from scanning radars and passive instruments. The nadir-pointing CPR provides only "instantaneous" vertical cross sections of hurricanes during CloudSat overpasses.

2. Description of Retrieval Methods

[7] The attenuation-based reflectivity gradient method for retrievals of rainfall from CPR measurements [*Matrosov et al.*, 2008] was used to estimate rain rates in the vertical atmospheric column. This method takes advantage of the low vertical variability of nonattenuated W band reflectivity in rain, which is usually true for stratiform rainfall, and strong attenuation of radar signals in this frequency band, so the vertical gradients of the measured equivalent radar reflectivity factor (hereafter just reflectivity), Z_{em}, in a liquid hydrometeor layer containing rain are shaped primarily by attenuation effects. The relative constancy of nonattenuated W band reflectivities is especially true for rain rates, R, that are greater than about 3–4 mm h^{-1}. At such rain rates, strong non-Rayleigh scattering effects result in changes of these reflectivities only in a relatively narrow interval of few decibels and the reflectivity variability due to raindrop size distribution (DSD) details is small [*Matrosov*, 2007]. The vertical gradients of observed reflectivity, which are used as a proxy for the attenuation coefficient, are then related to rain rates at a height h, $R(h)$ [*Matrosov et al.*, 2008],

$$R(h) = 0.5k(h)\beta[\partial Z_{em}(h)/\partial h]_c - G(h), \qquad (1)$$

where the dimensionless coefficient $k(h)$ accounts for the changes in air density, ρ_a [$k(h) = 1.1\rho_a(h)^{0.45}$, $\rho_a(h)$ in kg m^{-3}], $\beta \approx 1.2$ if the reflectivity gradients and rain rates are in dB km^{-1} and mm h^{-1}, respectively, and the term $G(h)$ accounts for the gaseous and cloud absorption. The gaseous absorption is accounted for using model calculations of water vapor and oxygen absorption assuming 95% relative humidity in the rain layer. To account for attenuation contributions from liquid water clouds coexisting with rain, it was assumed that the mean cloud liquid water content (LWC) is 0.25 g m^{-3}. This value is consistent with experimental in situ observations in precipitating clouds [e.g., *Mazin and Khrgian*, 1989] and with remote sensing estimates from ground-based observations [*Matrosov*, 2009, 2010b]. Cloud LWC and the cloud absorption coefficient are linearly related [e.g., *Stepanenko et al.*, 1987].

[8] The subscript c at the derivative sign in (1) denotes that the derivative value is corrected for multiple scattering (MS) effects. These effects are present in CloudSat measurements due to a relatively large footprint of the CPR (~1–1.5 km near the ground). They cause an increase in the observed reflectivity values compared to those that would be measured in the case of single scattering [e.g., *Battaglia et al.*, 2008]. Multiple scattering changes the absolute reflectivities significantly, but the reflectivity vertical gradients are influenced only weakly. A correction procedure to account for MS effects in the attenuation-based reflectivity gradient method for $R < 20$ mm h^{-1} in stratiform-like rainfall retrievals was described by *Matrosov et al.* [2008].

[9] Rain rate retrievals are performed in the liquid hydrometeor layer. In stratiform-like rainfall, CPR reflectivities usually exhibit a peak (i.e., a bright band (BB)) in the melting region located just below the 0° isotherm [*Sassen et al.*, 2007; *Matrosov*, 2008]. This peak signature can be used for separating the liquid hydrometeor layer containing rain from the ice dominating cloud parts. Melting hydrometeors are typically present in a layer which is about 0.5–0.6 km thick and is located below the 0° isotherm. To ensure that rainfall estimates are not affected by melting hydrometeors, the upper boundary of the rain rate retrievals was set to a 600 m height bellow the freezing level (i.e., the 0° isotherm). Stratiform-like rainfall areas are often present in hurricane observations (except the regions of stronger convection) as was observed in TRMM studies [e.g., *Yokoyama and Takayabu*, 2008] and as will be shown for CloudSat observations in section 3.

[10] The rain rate retrieval errors using the attenuation-based gradient method are primarily influenced by the vertical variability of nonattenuated W band reflectivity in rainfall, variability of the coefficient β in the attenuation-rain rate relations (see (1)) and uncertainties in the gaseous and cloud absorption. These errors are estimated at about 40%–50% [e.g., *Matrosov*, 2007] for stratiform-like rainfall. They can be higher for rainfall estimates in convective regions.

[11] Attenuation of the radar signals in ice regions of precipitating systems above the BB is usually much smaller

than that in the liquid and melting hydrometeor layers. The radar reflectivities above the BB are dominated by returns from ice particles. The ice water content (IWC) and its vertical integral, ice water path (IWP), of the cloud regions observed above the BB are estimated from measured reflectivity, using the empirical IWC-Z_e relations. Some MS effects are also present in CloudSat measurements in ice regions. The reflectivity increase due to MS, however, is approximately balanced out by some modest attenuation in dry ice cloud phase. As a result, the CPR reflectivities observed above the BB might be considered as a proxy to the single scattered nonattenuated reflectivities [*Matrosov and Battaglia*, 2009].

[12] CPR-observed reflectivities of ice regions of precipitating systems (including hurricanes) are usually very high (up to 20 dBZ or so). An IWC-Z_e relation specifically developed for high reflectivity ice cloud regions and W band reflectivity [*Matrosov and Heymsfield*, 2008] was further used in this study,

$$\mathrm{IWC}\left(\mathrm{g\ m^{-3}}\right) = 0.086\ Z_{\mathrm{em}}^{0.92}\left(\mathrm{mm^6 m^{-3}}\right). \qquad (2)$$

[13] This relation accounts for nonsphericity of ice/snow particle aggregates and non-Rayleigh scattering effects. The temperature dependence of the coefficients in the IWC-Z_{em} relations is not significant for higher reflectivities values, which are typical for precipitating systems. Uncertainties of ice mass estimates using reflectivity measurements could be as large as a factor of 2 or even higher [e.g., *Protat et al.*, 2007; *Matrosov and Heymsfield*, 2008]. When calculating IWP as a summation of IWC along the vertical, a partial cancelation of errors can be expected when at least part of the IWC error is random so it has opposite signs at different heights.

[14] Satellite-based approaches for estimating cloud ice water path from passive microwave measurements have been developed in the past [e.g., *Liu and Curry*, 1999]. IWP retrieval errors from radar measurements could be comparable to those from multifrequency passive measurements. For ice cloud retrievals at the Southern Great Plains instrumented site, *Seo and Liu* [2005] reported a generally good agreement between IWP estimates from ground-based radar using the IWC-Z_{em} relations and IWP retrievals from upwelling brightness temperatures. These authors used radar information to improve passive retrievals and generally considered precipitation free areas. The presence of rainfall generally complicates passive retrievals but does not affect the nadir-pointing radar measurements of ice regions in precipitating systems. CloudSat measurements provide an opportunity for high-resolution retrievals of IWP and resultant rainfall in the same vertical atmospheric column.

3. CloudSat Observations of Hurricane Gustav

[15] Hurricane Gustav was one of the major hurricanes of the 2008 season. It formed on 25 August about 400 km southeast of Haiti. It reached category 4 strength when entering the Gulf of Mexico, then lost some of its intensity and was a category 3 hurricane for most of the time while crossing the Gulf. Just before the landfall at around 1400 UTC (1 September 2008) near Cocodrie, LA (N29°14′49″, W90°39′41″), it weakened to a category 2 hurricane. Gustav caused at least $8.5 billion in total damages and triggered the largest population evacuation in U.S. history. While this hurricane also made landfalls in Haiti and Cuba on its way to the U.S. mainland, observations made close to the time of the landfall on the Louisiana coast are of the main interest for this study, because they have supporting measurements including rainfall estimates from the Weather Surveillance Radar-1988 Doppler (WSR-88D) network.

3.1. CloudSat Observations of Hurricane Gustav Near Landfall

[16] The CloudSat passed over Gustav on the descending orbit at around 800 UTC on 1 September 2008, which is about 6 h prior to the official landfall time. Figure 1a shows the rainfall reflectivity map as measured by the New Orleans WSR-88D radar, which has a four-letter identifier KLIX, at the lowest elevation angle. The WSR-88D radars have a beam width of about 1° and operate at S band frequencies, which usually are only negligibly attenuated in rain. These radar wavelengths λ of about 11 cm are large enough compared to most atmospheric hydrometeor particles, so values of Z_e in Figure 1a can be considered as nonattenuated Rayleigh scattering reflectivities. The spiral rainbands are seen in KLIX measurements, as the hurricane approaches New Orleans. The CloudSat overpass occurred almost directly over the KLIX radar, which makes direct CloudSat-WSR-88D comparisons convenient.

[17] The observed nadir pointing CPR reflectivities during the overpass are shown in Figure 1b. CloudSat reveals the cross section of the hurricane as it passes along the track shown by the white line in Figure 1a. The cloud tops reach heights of about 16 km above mean sea level (MSL). The area of rainfall is clearly identifiable between latitudes of about 28° and 29.8° by strong vertical gradients of reflectivity diminishing toward the ground. For most rainfall, CPR ground returns are not seen, although observed reflectivities remain above the radar sensitivity limit even near the ground, indicating the presence of MS effects in return echoes. While significantly enhancing observed CPR reflectivities everywhere in the liquid hydrometeor layer, these effects change the vertical gradient of reflectivity to much lesser extent. The gradient change is accounted for by the MS correction [*Matrosov et al.*, 2008].

[18] The radiosonde soundings conducted at 0000, 0600 and 1200 UTC on 1 September 2008 from a location near KLIX indicated that the height of the 0° isotherm was at 4.8–4.9 km MSL. It can be seen from Figure 1b that the BB features, which separate the liquid hydrometeor layer and the layer dominated by the ice phase, are identifiable for most of the reflectivity cross section where rain is present. The signal attenuation above the BB is not obvious, suggesting predominantly the ice phase and little liquid water, which causes much stronger attenuation of W band radiation than ice. The exception is the region between latitudes of about 28.6° and 29° where the attenuation is indefinable in the relatively thin layer above the 0° isotherm and the BB features are not seen. This is likely due to some convection activity, which brought a substantial amount of liquid above the freezing level in updrafts. No strong convective cores corresponding to undiluted convection, however, are obvious along the CloudSat track. The fact that tropical precipitation (including tropical cyclones) has a substantial stratiform component

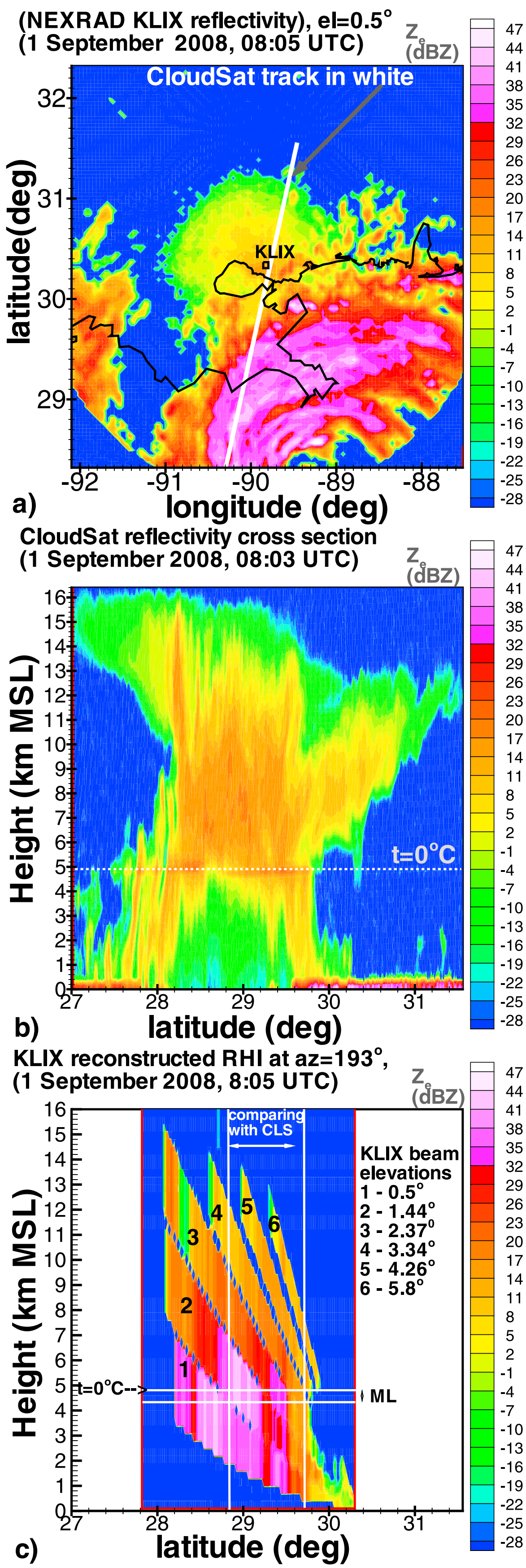

is, however, very common [e.g., *Houze*, 1997; *Yokoyama and Takayabu*, 2008].

[19] CloudSat passed almost directly over a ground-based precipitation radar in a hurricane, which is a relatively rare coincidence. Given this, it is instructive to compare the cross section of Gustav as seen by the CPR (Figure 1b) with a corresponding cross section as seen by the KLIX radar. While WSR-88D radars do not perform range-height indicator (RHI) scans to provide such cross sections directly, low-resolution RHI data can be obtained from a set of azimuthal scans.

[20] For the same spatial scale as in Figure 1b, Figure 1c shows a KLIX low-resolution RHI cross section in the vertical plane of the CloudSat track. This cross section was reconstructed from data collected during six azimuthal scans at elevations of 0.5°, 1.44°, 2.37°, 3.34°, 4.26°, and 5.8°. Six KLIX beams (which become broader with range) corresponding to these elevations are clearly seen in Figure 1c. The beam broadening effects, which are in part due to the curvature of the Earth and refraction, were accounted for using techniques from the work of *Doviak and Zrnic* [1993]. The position of the melting layer in Figure 1c is shown by the horizontal white lines, for a typical BB thickness.

[21] It is interesting to note that the KLIX radar resolves some of the features in the ice part of the hurricane seen by the CPR (e.g., the tower-like region of strong ice reflectivity centered at latitude of about 28.2°). The corresponding KLIX S band reflectivities in this region are, however, stronger than those from the CPR (19–20 dBZ versus 14–15 dBZ). A 5 dB S–W band reflectivity difference corresponds to approximately 1.5 mm size ice crystals if this difference is attributed to nonRayleigh scattering at W band.

[22] It can be seen from Figure 1c that the upper part of the lowest 0.5° KLIX beam begins to penetrate into the melting layer at latitudes to the south of 28.85°, so KLIX measurements beyond this latitude are "contaminated" by melting ice hydrometeors and are not directly representative of rainfall. This fact is manifested by the area of increased reflectivity in the lowest beam data between latitudes of about 28.5° and 28.85°. The melting layer "contamination" is also clearly seen in the 1.44° KLIX beam between about 28.85° and 29.2°. Judging from both CloudSat and KLIX measurements (Figures 1b and 1c), there is no significant rainfall to the north of latitude ~29.7°. From this, it can be concluded that comparing rainfall estimates from CloudSat and KLIX data only make sense in the latitude interval ~28.85°–29.7°.

[23] A part of the CloudSat measurements corresponds to observations over land (areas to the north of the 29.2° latitude) and the rest correspond to observations over water. Figure 2a shows comparisons of CloudSat and KLIX rainfall estimates along the satellite ground track. The generic S band NEXRAD Z_e-R relation ($Z_e = 300R^{1.4}$, where Z_e is in mm^6 m^{-3} and R is in mm h^{-1}), which is customarily applied for quantitative precipitation estimations (QPE) with

Figure 1. (a) The reflectivity map of the WSR-88D KLIX radar at the time of the CloudSat overpass of hurricane Gustav just prior to its landfall, (b) the corresponding time-height cross section of the CloudSat data, and (c) the reconstructed KLIX RHI in the direction of the CloudSat track.

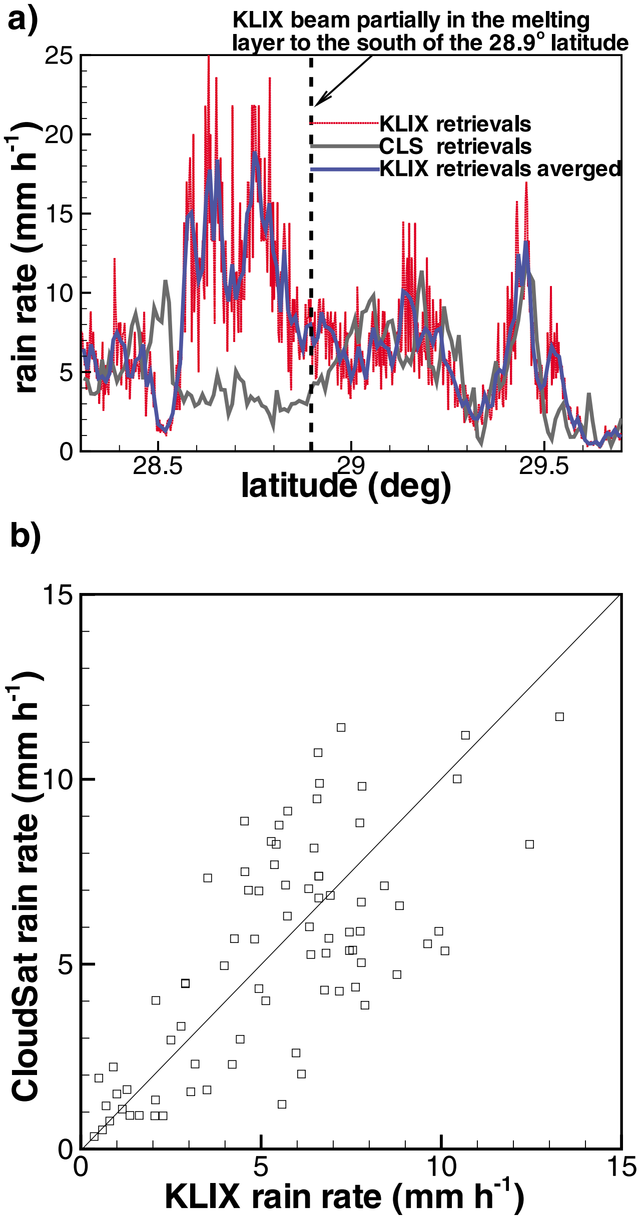

Figure 2. (a) Comparisons of the hurricane Gustav rain rates retrieved from CloudSat measurements and from the WSR-88D KLIX radar measurements (original resolution and averaged KLIX data are shown) sampled along the satellite track (1 September 2008, 0801 UTC) and (b) the scatterplot of CloudSat and averaged KLIX data for latitudes north of 28.9°.

WSR-88D radars [e.g., *Krajewski et al.*, 2010], was used with KLIX measurements. Note that original KLIX measurements are somewhat noisy. The increased noise in the WSR-88D radar measurements (as compared to the legacy resolution mode measurements with radial sampling using a 1 km resolution) is caused in part by the transition to the super resolution mode with a 250 m gate sampling along the radial, which is now often used with these radars. To simplify comparisons, the original WSR-88D retrievals were averaged over 1.5 km to better match the CPR resolution. These averaged retrievals are also shown in Figure 2a.

[24] The retrievals from CloudSat measurements in Figure 2a correspond to the mean rain rates in a layer which is matched with the KLIX vertical resolution. Averaging of vertically resolved CloudSat retrievals was performed for more direct comparisons. The KLIX radar beam is about 1.5–2.5 km wide in the region of comparisons and the KLIX sampled area is located progressively higher above the ground as the range from the radar increases (see Figure 1c).

[25] The agreement between CloudSat and KLIX estimates of rainfall in the area to the north of 28.85° in Figure 2a is good given the inherent retrieval uncertainties of both approaches. The uncertainties of reflectivity based estimates of rain rate for S band radars are quite significant [e.g., *Doviak and Zrnic*, 1993] and could be comparable to the uncertainties of the CloudSat retrievals or even higher. *Krajewski et al.* [2010] indicated that WSR-88D rainfall accumulation estimates can differ from gauge measurements by as much as a factor of almost 2. Both retrieval estimates clearly indicate a prominent minimum at around 29.3°–29.4° (just inland from the coast) between two distinct rainfall bands. It can also be seen that to the south of 28.9° in Figure 2a, the agreement between the Cloudat and KLIX rain rate estimates is poor due to the aforementioned melting layer contamination of the WSR-88D data. The scatterplot of CloudSat and KLIX averaged rain rates along the satellite track for latitudes to the north from 28.9° are shown in Figure 2b. The correlation coefficient between these two types of retrievals is 0.72. CloudSat estimates were on average a little smaller (the relative bias is −8%), and the relative standard deviation between satellite and ground-based estimates is about 54%.

[26] Multiple scattering effects, which were accounted for in CloudSat retrievals, make the observed CPR reflectivity gradients less steep (compared to the single scattering gradients). Ignoring these effects could result in underestimating retrieved rainfall. The MS corrections increase with rainfall rate (and the distance from the melting layer) and are about 12%–15% for the considered rain layer freezing level heights of about 5 km and typical retrieved values of R around 5–6 mm h^{-1}. For maximum CloudSat-derived rain rates (for this comparison) of about 10–12 mm h^{-1}, these corrections are about 25%. Note that while the MS corrections are generally less than retrieval uncertainties, they need to be introduced (at least for R > 5 mm h^{-1} or so), otherwise the CloudSat retrievals might exhibit a negative bias. While MS corrections were initially developed for stratiform rainfall [*Matrosov et al.*, 2008], they were also applied here for the region of mild convection between latitudes 28.6° and 29°.

[27] The comparisons presented in Figure 2a also indicate an important utility of the CloudSat measurements of rainfall in coastal areas when they allow continuous high horizontal spatial resolution (~1.5 km) rainfall retrievals along the satellite track, while WSR-88D radars are limited in range by 150 km or so. This limitation of the WSR-88D Next Generation Weather Radars (NEXRAD) exist because their beams begin to encounter melting hydrometeors (even for the lowest elevation angles and the highest freezing levels), and thus these radar measurements for longer ranges are not directly representative of rainfall below the melting layer.

[28] Figure 3 shows the results of total ice mass retrievals along the hurricane Gustav track. The corresponding IWP

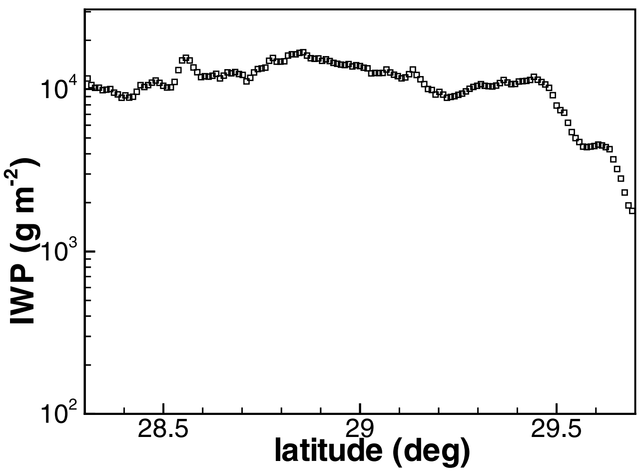

Figure 3. CloudSat retrievals of IWP in hurricane Gustav on 1 September 2008, 0801 UTC, just prior to its landfall.

values were obtained by the vertical integration of IWC estimates, which were retrieved at each CloudSat vertical resolution gate above 5 km MSL. For a given latitude, these IWP values and estimated layer mean values of rain rate, as shown in Figure 2a, correspond to the same measurement profiles, thus CloudSat observations allow characterization of different hydrometeor information in the same vertical column during stratiform precipitation.

[29] While in the regions of the identifiable melting layer (i.e., the bright band), an assumption that reflectivity above the BB is dominated by ice hydrometeor is likely justified, in the areas of convection (e.g., between 28.6° and 29°) it might not be exactly so, at least up to the heights of about 5.5 km MSL where noticeable attenuation of measured Z_e is observed. There is no discontinuity, however, in the retrieved values of IWP which do not show significant variability along the satellite track in the regions where rainfall is present. It should be mentioned also that more than 90% (on average) of the total columnar IWP in these regions comes from the heights greater than 5.5 km MSL where there are no obvious signs of signal attenuation.

[30] As seen from Figure 3, typical values of IWP in hurricane Gustav just prior to landfall were about 10^4 to 2×10^4 g m^{-2} or so. They were rapidly diminishing in the areas where the hurricane core had not yet arrived and rainfall was weak or absent (i.e., north of 29.5°). Because of its high sensitivity (~−28 dBZ) and negligible attenuation in the upper parts of the echo, the CPR detects what could be considered cloud tops, so presented IWP values practically correspond to whole vertical extent of the hurricane system. In case of other spaceborne radars (e.g., the TRMM PR), the total ice estimates could be significantly underestimated due to a lower radar sensitivity (i.e., about 17 dBZ for the TRMM PR) resulting in much lower altitudes of smallest detectable echoes.

3.2. CloudSat Observations of Remnants of Hurricane Gustav

[31] After the landfall on 1 September 2008, Gustav moved inland and weakened to a tropical storm that evening and to a tropical depression the next day. It took a generally northern direction through Arkansas and was again observed by CloudSat as a precipitating extratropical system over eastern Kansas and north–western Missouri on 4 September 2008. Figure 4a shows a WSR-88D radar reflectivity map at the time when CloudSat was passing over this system on the descending orbit at around 0832 UTC. This WSR-88D radar has the four-letter identifier KEAX and is located near Kansas City, MO. It was the closest WSR-88D radar for this overpass.

[32] The corresponding time-height cross section of CloudSat measurements is shown in Figure 4b. It can be

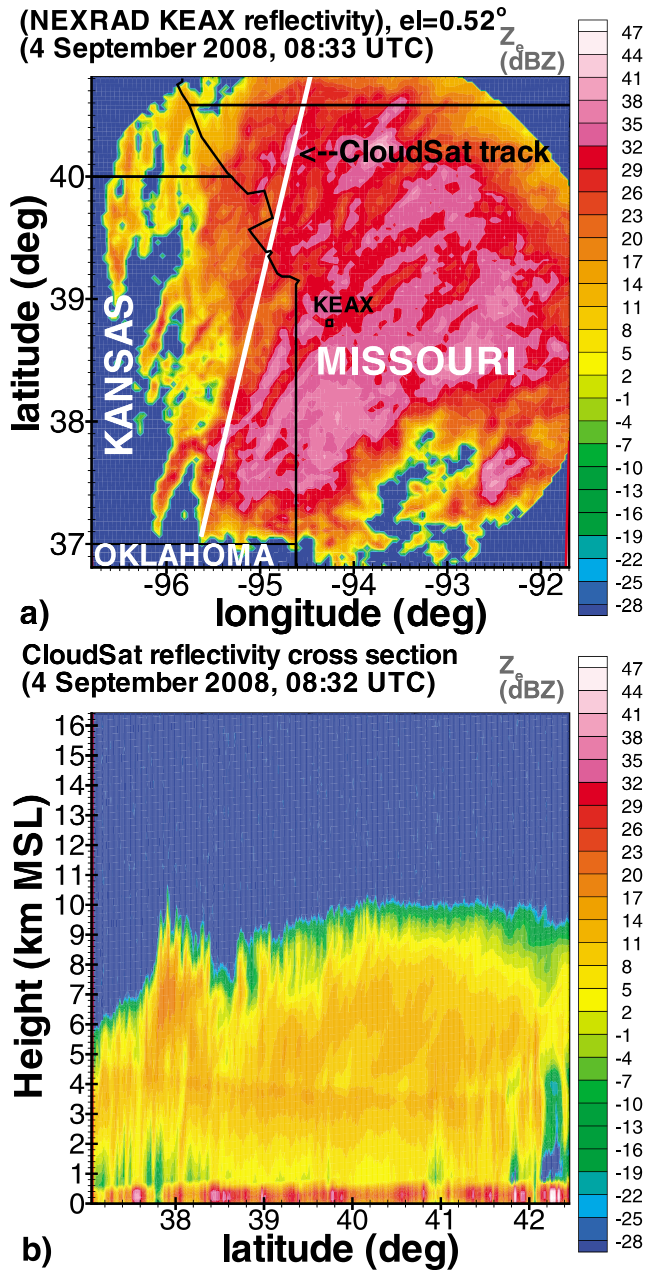

Figure 4. (a) The reflectivity map of the WSR-88D KEAX radar at the time of the CloudSat overpass of remnants of hurricane Gustav on 4 September 2008 and (b) the corresponding time-height cross section of the CloudSat data.

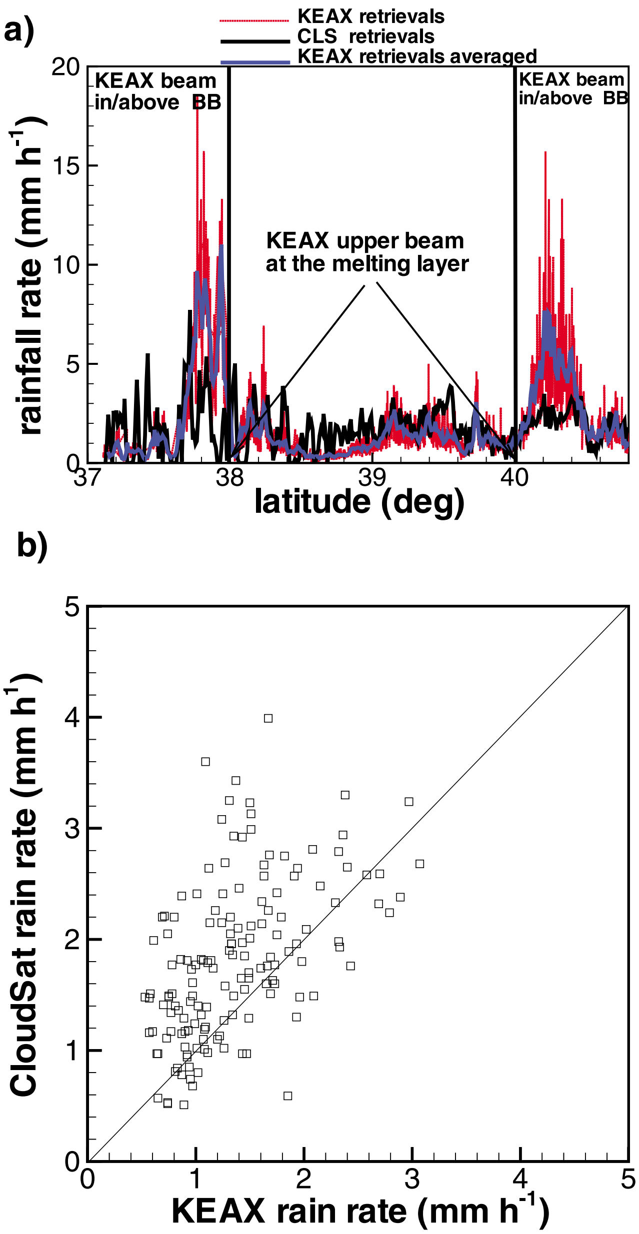

Figure 5. (a) Comparisons of the hurricane Gustav remnants rain rates retrieved from CloudSat measurements and from the WSR-88D KEAX radar measurements (original resolution and averaged KEAX data are shown) sampled along the satellite track (4 September 2008, 0832 UTC) and (b) the scatterplot of CloudSat and averaged KEAX data between latitudes 38° and 40°.

seen from Figure 4b that the observed remnants of hurricane Gustav look more like a classical stratiform precipitating system with clearly identifiable bright band features. The bright band altitude gradually becomes higher as the satellite moves south. It is centered at around 3.6 km MSL at latitude of 42.5° and at about 4.1 km MSL at 37°. The cloud top echoes are observed at a height of about 10 km MSL. The ground returns are seen for the entire duration of the overpass, although the CloudSat PIA-based rainfall retrieval technique cannot be used because these returns are from land surfaces.

[33] Figure 5a shows comparisons of layer mean rain rate retrievals from CloudSat using the attenuation-based reflectivity gradient method with KEAX estimates sampled along the satellite ground track. As for comparisons near the hurricane Gustav landfall, the same assumptions for CloudSat retrievals were made and the standard NEXRAD Z_e-R relation ($Z_e = 300R^{1.4}$) was used with the KEAX data. The KEAX radar beam was fully within the rain layer for the comparison interval between the latitudes of about 38° and 40°, so sensible comparisons can be performed only in this interval. Beyond this interval, which is marked in Figure 5a by solid vertical lines, the KEAX measurements have obvious artifacts caused by the melting layer reflectivity enhancements that are followed by measurements in ice/snow regions at further distances.

[34] Typical rain rates for this event in the comparison interval were around 2 mm h^{-1}. Overall the agreement between ground-based and spaceborne estimates for this comparison is within retrieval uncertainties of both approaches. The corresponding scatterplot for rainfall estimates from CloudSat and averaged data from KEAX between 38° and 40° is shown in Figure 5b. The correlation coefficient between two data sets is 0.43. The CloudSat estimates were on average larger than those from KEAX by 31%, and the relative standard deviation between satellite and ground-based retrievals is 56%.

[35] Despite the fact that the MS effects on the reflectivity gradients in the rain layer are expected to be negligible for light rainfalls [*Matrosov et al.*, 2008], the CloudSat retrievals at such low rain rates are likely to have higher uncertainties (~50–60% or so) compared to the satellite data in Figure 2 due to general weakness of rain attenuation. The more significant noise of the CloudSat retrievals in Figure 5a compared to Figure 2a is likely to be a consequence of these higher uncertainties.

[36] The retrieved values of IWP for the precipitating cloud system caused by remnants of hurricane Gustav is shown in Figure 6. These values are generally smaller than those for

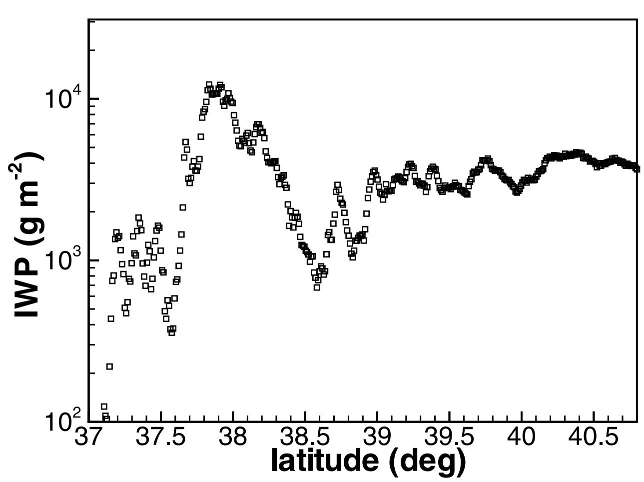

Figure 6. CloudSat retrievals of IWP in hurricane Gustav remnants on 4 September 2008, 0832 UTC.

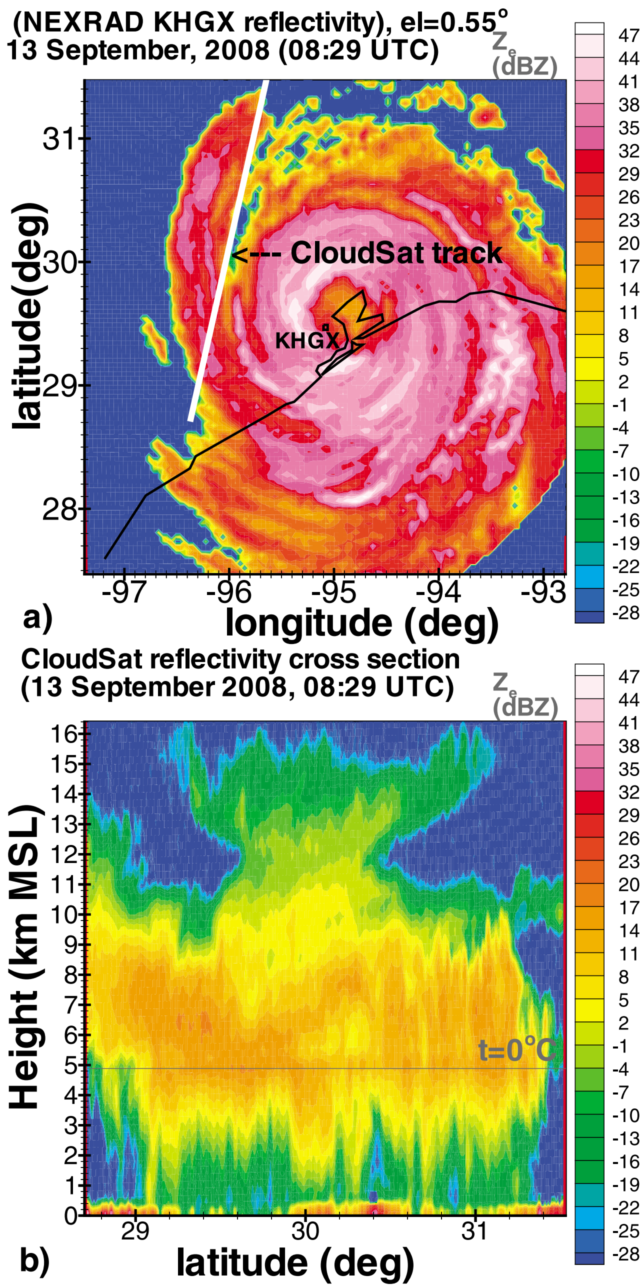

Figure 7. (a) The reflectivity map of the WSR-88D KHGX radar at the time of the CloudSat overpass of hurricane Ike just after its landfall and (b) the corresponding time-height cross section of the CloudSat data.

the hurricane just prior the landfall (see Figure 3) except a maximum at latitude of about 38°, which produces IWPs comparable with those at the time of the hurricane landfall. This maximum is caused by a tower-like feature seen at this latitude in the CloudSat reflectivity measurements in Figure 4b. While this feature is not very high, the reflectivities in its core (at around 7 km MSL) are very strong (~20–22 dBZ), which exceeds maximum observed reflectivities in ice regions during this hurricane landfall (Figure 1b). This feature, however, does not cause significant attenuation, which, in part, is evident from the presence of the ground returns, and it, most likely, consists of large ice/snow particles at relatively high concentrations. The variability in IWP to the north of the 39° latitude is relatively minor.

4. CloudSat Observations of the Landfall of Hurricane Ike

[37] Hurricane Ike, which followed hurricane Gustav in the Gulf of Mexico about 2 weeks later, was the third most destructive hurricane to ever make landfall in the United States (after hurricane Andrew in 1992 and hurricane Katrina in 2005). It had a maximum strength of category 4 and caused more than \$30 billion in total damages and resulted in at least 195 human deaths (112 in the United States). At its peak on 4 September, with sustained winds of about 230 km h^{-1}, Ike was the most intense hurricane of the 2008 season. It made its final landfall east of Galveston, TX, as a category 2 hurricane on 13 September 2008 at around 0710 UTC.

[38] CloudSat crossed over the western part of Ike on a descending orbit a little more than 1 h after the landfall (~0829 UTC). A WSR-88D reflectivity measurement map of Ike at the time of the crossing is shown in Figure 7a. These measurements at the lowest elevation angle of 0.55° were made by the Houston, TX, WSR-88D radar, which has the four-letter identifier KHGX. The eye of the hurricane over the Galveston Bay is clearly seen in this reflectivity map just to the northwest of the KHGX radar location. The maximum WSR-88D reflectivities of hurricanes Ike and Gustav are comparable (~50 dBZ). However, in the case of Ike (as opposed to Gustav), CloudSat passed over one of the outer rainbands, which had lower reflectivities and thus lighter rainfall. The closest point of this overpass from the KHGX radar was at a distance of about 100 km.

[39] The cross section of the CloudSat observations that correspond to this overpass, which occurred over the land surface, is shown in Figure 7b. The melting layer BB features are clearly visible for practically the entire overpass north of the 29° latitude, and the rainfall layer attenuation patterns are aligned vertically almost perfectly indicating a stratiform-like rainfall in this rainband. The ground returns were detected for most of the crossing. The height of the freezing level (i.e., the 0° isotherm) during the Ike landfall was very similar to that of the landfall of hurricane Gustav (i.e., ~4.9 km MSL). While cloud top echoes in the middle of the CloudSat overpass reached heights of about 16 km MSL, which is similar to hurricane Gustav in Figure 1b, in pockets of this peripheral rainband, cloud top heights were significantly lower.

[40] The comparisons of CloudSat and WSR-88D rainfall estimates for the hurricane Ike landfall case make sense for the interval between latitudes of about 29° and 30°. In the region to the north of about 30°, CloudSat observes the very edge of the rainband where significant horizontal gradients of rainfall and cloud properties are likely, and there is little rainfall observed along the CloudSat ground track in the region to the south of 29°. Besides, in this region the KHGX radar beam begins to be influenced by the melting layer beyond distances of about 150–160 km even at the lowest radar elevation angle (~0.5°) due to the Earth's curvature and atmospheric refraction. As a result, the WSR-88D

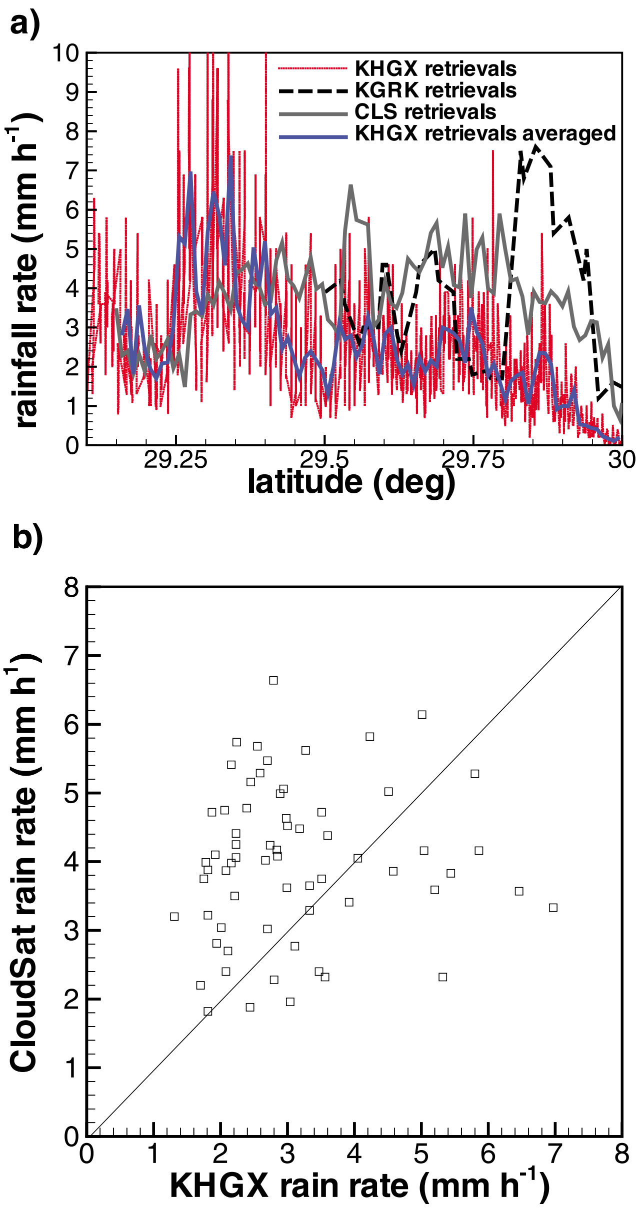

Figure 8. (a) Comparisons of the hurricane Ike rain rates retrieved from CloudSat measurements and from the WSR-88D radar measurements (original resolution and averaged KHGX data are shown) sampled along the satellite track (13 September 2008, 0829 UTC) and (b) the scatterplot of CloudSat and averaged KHGX.

data there have artifacts caused by the BB reflectivity enhancements.

[41] For the hurricane Ike landfall overpass, the CloudSat rainfall retrievals are compared to the WSR-88D estimates in Figure 8a. The agreement between CloudSat and KHGX derived rain rates is very good up to latitude of about 29.35°. Beyond this latitude, CloudSat estimates are generally greater than those from the KHGX radar. This is not very surprising given the retrieval uncertainties and also a relatively long distance from the KHGX radar location and the comparison region (~100–110 km). Overall, for the comparison interval, the CloudSat rain rate estimates are greater than averaged KHGX data by about 26% and the relative standard deviation is 57%. The corresponding scatterplot is shown in Figure 8b.

[42] The CloudSat ground track for the hurricane Ike landfall event was also within a reach from another WSR-88 D radar located near Austin, TX. Although this radar, which has the four-letter identifier KGRK, is located further from the areas of CloudSat retrievals, its estimates are also shown in Figure 8 for the interval where the KGRK-CloudSat ground track distance differences were less than 160 km. Unlike the KHGX radar, which operated in the super resolution mode (i.e., at a 250 m radial resolution), the KGRK radar operated in the legacy resolution mode (i.e., at a 1 km radial resolution). As a result, the KGRK rain rate estimates are less noisy than those from the KHGX radar. The agreement between the KGRK and KHGX estimates is generally good except for latitudes between 29.8° and 30°. One possible explanation of the peak in the KGRK estimates in this latitude interval is that atmospheric refraction was stronger than average and some BB contamination of the KGRK data in these directions took place at shorter distances than usual.

[43] Figure 9 shows CloudSat-based IWP retrievals along the satellite ground track. As for the hurricane Gustav landfall case, IWP values were calculated by the vertical integration of IWC obtained from CloudSat reflectivities at heights above 5 km MSL. There were no obvious convective regions in the outer rainband of hurricane Ike crossed by CloudSat so reflectivities observed above the melting layer are very likely to be dominated by ice hydrometeors. No significant attenuation of radar signals is obvious in the ice part of the system, which is also indicative of the absence of significant amounts of liquid water above 5 km MSL.

[44] While the observed cloud tops were not the highest for latitudes less than about 29.4° in the hurricane Ike case, IWPs for these latitudes were greatest due to the large ice core with high reflectivities (up to 20 dBZ or so) centered between 5.5 and 7.5 km MSL. Overall the retrieved IWP values shown in Figure 9 are smaller than those in hurricane Gustav CloudSat retrievals (Figure 3), although the difference here can be attributed (at least in part) to the fact that the central regions of the hurricane with heavier rainfall were not observed by the CPR in the case of Ike (as opposed to Gustav). The variability of retrieved IWP increases to the

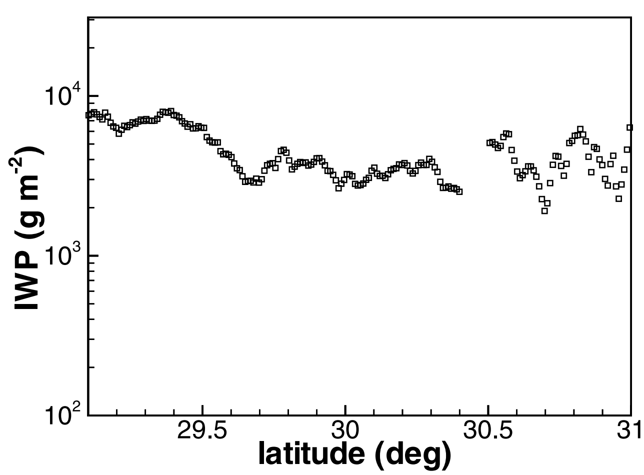

Figure 9. CloudSat retrievals of IWP in hurricane Ike on 13 September 2008, 0829 UTC.

north of 30.5°, probably due to the fact that CloudSat passes over the edge of the rainband.

5. Conclusions

[45] Although satellite observations of hurricanes have been conducted for decades, CloudSat offers some new opportunities for their spaceborne studies. Because of its high sensitivity, the first spaceborne W band cloud profiling radar (CPR) onboard CloudSat is able to resolve hurricane structures from the cloud tops at heights greater than 16 km MSL downward to the rain layer below. While CPR lacks spatial coverage, due to the nature of its nadir-pointing measurements, it provides a detailed view of vertical cross sections of hurricanes allowing quantitative estimates of rainfall and ice mass. Such a complete vertical view is not available either from passive (visible, IR, and microwave) satellite measurements or from the TRMM radar, which due to its limited sensitivity (about 17 dBZ) is not able to observe the upper parts of hurricanes.

[46] While CloudSat measurements of rainfall are influenced by multiple scattering effects, these effects can be approximately corrected for, and retrievals of rain rates (especially for rainfalls exhibiting bright band radar features outside areas of strong convection) inside hurricanes can be performed if a sufficient number of not contaminated by surface returns CloudSat range gates (≥3) are within the liquid hydrometer layer. These retrievals are generally available for $R < 20$ mm h^{-1} or so, and strong MS effects make CloudSat rainfall retrievals impractical for heavier rainfalls. The radar attenuation-based reflectivity gradient approach for rainfall retrievals is applicable regardless of the availability of the surface radar returns and thus can be used for observations over both land and water surfaces. Coupled with this approach, the CPR absolute reflectivity based methods for retrieving ice parts of precipitating systems provide estimates of ice content of hurricanes in the same vertical atmospheric column when the radar BB features are present.

[47] In addition to the lack of spatial coverage, another significant limitation of current spaceborne W band hurricane measurements is a relative rarity of CloudSat crossings over tropical cyclones. Crossings also may occur not over the regions of the most interest. These issues may make CPR observations better suited for research activities rather than for operational use. Continuous remote sensing estimates along the CloudSat track can provide valuable information for validating hurricane models. This could be especially important for studies of hurricane landfalls when the conditions change sharply, and hurricanes undergo rapid transformations. By providing vertically resolved high-resolution information on ice and rainfall regions of precipitating systems, CloudSat retrievals can also be useful for calibrating and refining remote sensing satellite techniques that have larger spatial coverage.

[48] This study provides illustrations of CloudSat measurements for two major hurricanes of the 2008 season. Examples are given for CloudSat overpasses of hurricanes Gustav and Ike that occurred within only a few hours of their landfall on the continental United States. In both cases, the CPR nadir-pointing measurements revealed detailed vertical cross sections of these hurricanes. The maximum cloud top echoes of both hurricanes were at about 16 km MSL. Radar bright band features at heights corresponding to just below the freezing level indicated the areas of stratiform-like precipitation. CloudSat retrievals showed that typical rain rates along the satellite pass were generally between 3 and 12 mm h^{-1}. A more central overpass of Gustav also showed an evidence of convective activities in some areas of retrievals. The remnants of Gustav, which were observed by CloudSat 3 days after this hurricane landfall, provided an example of a more classical wide-spread stratiform precipitating system with lower rain rates.

[49] Quantitative comparisons between CloudSat-derived mean rain rates in the liquid hydrometeor layer along the hurricane overpasses and approximately coincident R estimates from different WSR-88D NEXRAD radars (when these radar observations came from rainfall) indicated agreement that was typically within retrieval uncertainties of satellite and ground-based approaches. The relative standard deviations between CloudSat and WSR-88D estimates were around 54%–57%. While not giving wider area coverage (like scanning NEXRAD radars), CloudSat rainfall measurements have the advantage of providing continuous and simultaneous rainfall and ice mass estimates above both water and land surface along the satellite ground track making retrievals outside the coverage by the WSR-88D radars. This could be important for observing hurricanes over coastal waters and during landfalls because NEXRAD measurements are influenced by melting hydrometeors at distances greater than about 150 km (even for lowest elevations), so WSR-88D rainfall estimates could not be accurate at such distances and traditional radar coverage of landfalling hurricanes just offshore is not adequate.

[50] Since CloudSat resolves the entire vertical extent of hurricanes, the estimated rain rates can be coupled with simultaneous retrievals of ice content in the regions above freezing level thus providing unique high-resolution information about different hydrometeors in the same vertical atmospheric column. The first spaceborne radar estimates of the total ice content in landfalling hurricanes showed that the largest values of IWP were about 10^4 to 2×10^4 g m^{-2} in the central parts of hurricane Gustav. Somewhat smaller IWP values were retrieved in an off center spiral rainband of hurricane Ike. In remnants of hurricane Gustav, IWP values were generally significantly lower (10^3 to 5×10^3 g m^{-2}) although some areas of increased IWPs ($\sim 10^4$ g m^{-2}) were also observed.

[51] Modeling studies indicate that hurricane rainfall can change very significantly upon landfall [e.g., *Kimball*, 2008]. It provides a challenge for forecasting of hurricanes during this most damaging stage of their evolution. High-resolution CloudSat observations may be useful for validating models predicting hurricane changes upon landfall.

[52] **Acknowledgment.** This study was funded through NASA Project NNX10AM35G.

References

Battaglia, A., S. Kobayashi, S. Tanelli, C. Simmer, and E. Im (2008), Multiple scattering effects in pulsed radar systems: An intercomparison study, *J. Atmos. Ocean. Tech.*, *25*, 1556–1567.

Chen, Y., and M. K. Yau (2003), Asymetric structures in a simulated landfalling hurricane, *J. Atmos. Sci.*, *60*(18), 2294–2312.

Doviak, R. J., and D. S. Zrnic (1993), *Doppler Radar and Weather Observations*, 562 pp., Academic, San Diego.

Durden, S. L., S. Tanelli, and G. Dobrowalski (2009), CloudSat and A-train observations of tropical cyclones, *Open Atmos. Sci. J.*, *3*, 80–92.

Haynes, J. M., T. S. L'Ecuyer, G. L. Stephens, S. D. Miller, C. Mitrescu, N. B. Wood, and S. Tanelli (2009), Rainfall retrieval over the ocean with spaceborne W band radar, *J. Geophys. Res.*, *114*, D00A22, doi:10.1029/2008JD009973.

Houze, R. A., Jr. (1997), Stratiform precipitation in regions of convection: A meteorological paradox? *Bull. Am. Meteorol. Soc.*, *78*, 2179–2196.

Kimball, S. K. (2008), Structure and evolution of rainfall in numerically simulated landfalling hurricanes, *Mon. Weather Rev.*, *131*, 687–697.

Krajewski, W. F., G. Villarini, and J. A. Smith (2010), Radar-rainfall uncertainties, *Bull. Am. Meteorol. Soc.*, *91*, 87–94.

Liu, G., and J. A. Curry (1999), Tropical ice water amount and its relations to other atmospheric hydrological parameters as inferred from satellite data, *J. Appl. Meteorol.*, *38*, 1182–1194.

Lonfat, M., F. D. Marks Jr., and S. S. Chen (2004), Precipitation distribution in tropical cyclones using the tropical rainfall measuring mission (TRMM) microwave imager: A global perspective, *Mon. Weather Rev.*, *132*, 1645–1660.

Luo, Z., G. L. Stephens, K. A. Emmanuel, D. G. Vane, N. D. Tourville, and J. M. Haynes (2008), On the use of CloudSat and MODIS data for estimating hurricane intensity, *IEEE Geosci. Remote Sens. Lett.*, *5*, 13–16.

Matrosov, S. Y. (2007), Potential for attenuation-based estimations of rainfall rate from CloudSat, *Geophys. Res. Lett.*, *34*, L05817, doi:10.1029/2006GL029161.

Matrosov, S. Y. (2008), Assessment of radar signal attenuation caused by the melting hydrometeor layer, *IEEE Trans. Geosci. Remote Sens.*, *46*, 1039–1047, doi:10.1109/TGRS.2008.915757.

Matrosov, S. Y. (2009), Simultaneous estimates of cloud and rainfall parameters in the atmospheric vertical column above the Atmospheric Radiation Measurement Program southern Great Plains site, *J. Geophys. Res.*, *114*, D22201, doi:10.1029/2009JD012004.

Matrosov, S. Y. (2010a), CloudSat studies of stratiform precipitating systems observed in the vicinity of the Southern Great Plains Atmospheric Radiation Measurement site, *J. Appl. Meteorol. Climatol.*, *49*, 1756–1765, doi:10.1175/2010JAMC2444.1.

Matrosov, S. Y. (2010b), Synergetic use of millimeter and centimeter-wavelength radars for retrievals of cloud and rainfall parameters, *Atmos. Chem. Phys.*, *10*, 3321–3331, doi:10.5194/acp-10-3321-2010.

Matrosov, S. Y., and A. Battaglia (2009), Influence of multiple scattering on CloudSat measurements in snow: A model study, *Geophys. Res. Lett.*, *36*, L12806, doi:10.1029/2009GL038704.

Matrosov, S. Y., and A. J. Heymsfield (2008), Estimating ice content and extinction in precipitating cloud systems from CloudSat radar measurements, *J. Geophys. Res.*, *113*, D00A05, doi:10.1029/2007JD009633.

Matrosov, S. Y., A. Battaglia, and P. Rodriguez (2008), Effects of multiple scattering on attenuation-based retrievals of stratiform rainfall from CloudSat, *J. Atmos. Ocean. Tech.*, *25*, 2199–2108, doi:10.1175/2008JTECHA1095.1.

Mazin, I. P., and A. H. Khrgian (Eds.) (1989), *Clouds and Cloudy Atmosphere. A Reference Book*, 648 pp., Hydrometeoizdat, Leningrad, Russ.

Mitrescu, C., S. Miller, J. Hawkins, T. L'Ecuyer, J. Turk, P. Partain, and G. Stephens (2008), Near real time applications of CloudSat data, *J. Appl. Meteorol. Climatol.*, *47*, 1982–1994.

Mitrescu, C., T. L'Ecuyer, J. Haynes, S. Miller, and J. Turk (2010), CloudSat precipitation profiling algorithm-model description, *J. Appl. Meteorol. Climatol.*, *49*, 991–1003.

Protat, A., J. Delanoe, D. Bouniol, A. J. Heymsfiled, A. Bansemar, and P. Brown (2007), Evaluation of ice water content retrievals from cloud radar reflectivity and temperature using a larger airborne in situ microphysical database, *J. Appl. Meteorol. Climatol.*, *46*, 557–572.

Sassen, K., S. Y. Matrosov, and J. Campbell (2007), CloudSat spaceborne 94 GHz radar bright bands in the melting layer: An attenuation-driven upside down lidar analog, *Geophys. Res. Lett.*, *34*, L16818, doi:10.1029/2007GL030291.

Seo, E. K., and G. Liu (2005), Retrievals of cloud ice water path by combining ground cloud radar and satellite high-frequency microwave measurements near the ARM SGP site, *J. Geophys. Res.*, *110*, D14203, doi:10.1029/2004JD005727.

Skwira, G. D., J. L. Schroder, and R. E. Peterson (2005), Surface observations of landfalling hurricane rainbands, *Mon. Weather Rev.*, *133*, 454–465.

Stepanenko, V. D., G. G. Schukin, L. P. Bobylev, and S. Y. Matrosov (1987), *Microwave Radiometry in Meteorology*, 284 pp., Hydrometeoizdat, Leningrad, Russ.

Stephens, G. L., et al. (2008), CloudSat mission: Performance and early science after the first year of operation, *J. Geophys. Res.*, *113*, D00A18, doi:10.1029/2008JD009982.

Tanelli, S., S. L. Durden, E. Im, K. S. Pak, D. Reinke, P. Partian, R. Marchand, and J. Haynes (2008), CloudSat's cloud profiling radar after 2 years in orbit: Performance, external calibration, and processing, *IEEE Trans. Geosci. Remote Sens.*, *46*, 3560–3573.

Tuleya, R. E., M. A. Bender, and Y. Kurihara (1984), A simulation study of the landfall of tropical cyclones, *Mon. Weather Rev.*, *112*, 124–136.

Yokoyama, C., and Y. N. Takayabu (2008), A statistical study on rain characteristics of tropical cyclones using TRMM satellite data, *Mon. Weather Rev.*, *136*, 3848–3862.

S. Y. Matrosov, Cooperative Institute for Research in Environmental Sciences, NOAA/Earth System Research Laboratory, R/PSD2, 325 Broadway, Boulder, CO 80305, USA. (sergey.matrosov@noaa.gov)